JOURNAL OF APPLIED ELECTROCHEMISTRY 24 (1994) 1206–1212

Electrolytic process optimization by simultaneous-modular flowsheeting

R. D. LA ROCHE*, M. A. STADTHERR, R. C. ALKIRE

Department of Chemical Engineering, University of Illinois, Urbana, IL 61801, USA

Received 28 October 1992; revised 16 December 1993

A procedure is described for computer-assisted optimization of an electrolytic process flowsheet. Material, energy, and economic balances for all process units were incorporated in a nonlinear optimization routine for predicting the minimum selling price based on a discounted cash flow rate of return on investment. The optimization utilized a simultaneous-modular approach which was incorporated into the public version of the Aspen flowsheeting package, and used an infeasible path convergence method based on successive quadratic programming procedures. Electrolyte vapour–liquid equilibrium data were estimated by the 'non-random two-liquid' model. The Lagrangian multipliers of the constraint equations were used to determine the sensitivity of the optimum to key process variables. The method was illustrated by evaluation of two process flowsheets for electrosynthesis of methyl ethyl ketone (MEK) from 1-butene based on pilot-plant performance reported in the patent literature.

List of symbols

A_c	cell cost factor ($\$\,cell^{-1}$)
A_H	heat exchanger cost factor ($\$\,m^{-2}$)
A_p	pump cost factor ($\$\,s\,l^{-1}$)
A_R	rectifier cost factor ($\$\,kVA^{-1}$)
A_T	tank cost factor ($\$\,l^{-0.5}$)
A_{cm}	cell maintenance factor ($\$\,A^{-1}\,y^{-1}$)
A_{cl}	cell labour ($\$\,cell^{-1}\,y^{-1}$)
A_{cw}	cooling water cost ($\$\,m^{-3}$)
A_e	electricity cost ($\$\,kWh^{-1}$)
A_m	membrane cost ($\$\,cell^{-1}\,y^{-1}$)
A_{om}	other maintenance factor, fraction of plant capital less cell cost
C_p	cooling water heat capacity ($kJ\,kg^{-1}\,°C^{-1}$)
H	operating hours per year
I_C	current to each cell (A)
I_{TOT}	total current to all cells (A)
L_A	Lang factor for auxiliaries
L_C	Lang factor for cells
L_R	Lang factor for rectifiers
N	number of cells in plant
Q	heat removal load ($kJ\,h^{-1}$)
R	production rate ($kg\,h^{-1}$)
ΔT_{cw}	cooling water temperature rise (°C)
ΔT_{LM}	cooler log mean temperature difference (°C)
U	heat transfer coefficient for cooler ($kW\,m^{-2}\,°C^{-1}$)
v_e	electrolyte flow to each cell ($l\,s^{-1}$)
v_C	cell voltage (V)
ϵ_R	rectifier efficiency
ρ	cooling water density ($kg\,m^{-3}$)
θ_T	surge tank residence time (s)

1. Introduction

During early stages of process development, the evaluation of various pathways for transforming feedstocks into desired products [1] represents an optimization problem since one seeks the *best* possible path. For electrochemical routes, efficient methods for early screening of process alternatives are important since pilot-scale laboratory data can be system-specific and thus inflexible to major changes in process concept once development activities are under way. In the present work, a method is described for linking preliminary electrochemical data (which demonstrate technical feasibility) to engineering models of process units in order to optimize the process flowsheet [2].

Optimization of individual electrolytic cells can be accomplished by several methods [3, 4]. In many cases operation is influenced by process units upstream and/or downstream from the cell [5]. Optimization of the entire process flowsheet is thus generally to be preferred [6]. Typical considerations include product separation from the cell effluent as well as recovery and recycle of electrolyte, solvent, unconverted reactants, and byproducts [7]. Flowsheet simulation methods require mathematical models of process units along with physical property data; their use in electrochemical applications has recently been described [8–10]. Examples of commercially available software with electrochemical capabilities include Aspen Plus (Aspen Technology, Inc.), Aspen/SP (Simulation Sciences, Inc.), and PRO/II (Simulation Sciences, Inc.). Physical property data for such applications may be estimated for pure

* Present address: Cray Research, Eagan, MN 55121, USA.

0021-891X

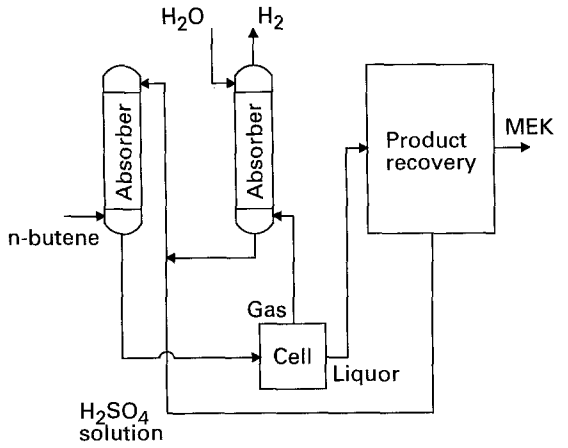

Fig. 1. Liquor recovery process flowsheet for electrosynthesis of methyl ethyl ketone.

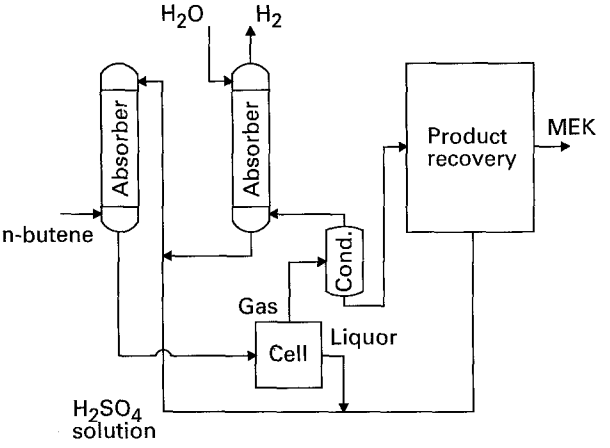

Fig. 2. Gas recovery process flowsheet for electrosynthesis of methyl ethyl ketone.

components by methods described by Reid *et al.* [11], and for liquid mixtures by the electrolyte nonrandom two-liquid (NRTL) model [12].

An electrochemical route to methyl ethyl ketone (MEK), outlined in patents by Worsham and coworkers [13, 14], has been identified as having the potential for achieving an overall reduction in energy requirements by comparison with conventional chemical routes [15]. Such a proposal is typical of over 2500 process concepts, usually fragmentary and only partially documented, that are available in the electrochemical patent literature [16]. A rational and efficient generic procedure for the engineering evaluation of such concepts is needed.

The purpose of this study was to establish a methodology for computer-aided design and optimization of electrolytic processes. The test cases used below to demonstrate the method were based on the patent literature and thus provided a zero-order base case.

2. Process modelling

The MEK patents [13, 14] represent a typical starting point for process evaluation. In this example, butanol is obtained by indirect hydration of 1-butene to 2-butanol, a fast second-order chemical reaction that proceeds quickly to equilibrium in an absorber [17].

$$C_4H_{8(g)} + H_2O \rightarrow C_4H_{10}O_{(aq)}$$

The butanol is fed to an undivided electrolytic cell where it is oxidized to MEK at 350 K and atmospheric pressure.

$$\text{Anodic:} \quad C_4H_{10}O_{(aq)} \rightarrow C_4H_8O_{(aq)} + 2H^+ + 2e^-$$

$$\text{Cathodic:} \quad 2H^+ + 2e^- \rightarrow H_2$$

The remainder of this section is segmented into two principal categories: 'process synthesis' (conception of promising process routes) and 'process flowsheeting' (simulation and optimization of process flowsheets).

2.1. *Process synthesis*

Figure 1 illustrates one possible processing route for the synthesis of MEK, referred to as the 'liquor recovery process'. This diagram represents the simple level which is typical of the patent literature; more complex flow sheets could also be analysed. Feedstock *n*-butene is absorbed in sulphuric acid and hydrated to 2-butanol which is fed to the electrolytic cell area. The effluent cell liquor (MEK and unreacted 2-butanol in concentrated sulphuric acid) passes to a product recovery section where MEK is separated by a distillation system. All other streams are recycled to the butene absorber. The effluent cell gas, which contains hydrogen, is scrubbed of volatiles which are returned to the absorber.

Figure 2 illustrates a second possible processing route, the 'gas recovery process', which takes advantage of the volatility of MEK. In this process, MEK is recovered via condensation of the cell gas in a refrigerated water cooler; liquid from the cooler proceeds to an azeotropic distillation to remove water, and then to a finishing column to achieve 99% product. The effluent hydrogen stream passes through a refrigerated water absorber to recover trace amounts of MEK and 2-butanol for recycling. The relatively pure hydrogen stream was credited as a byproduct fuel gas. This process route has the advantage of a simplified recovery section. The 'gas recovery process' would require a high partial pressure of MEK, to be achieved by operating with a high MEK concentration in the liquid recycle stream. It had been noted in the patent literature [13, 14] that MEK concentrations up to 22 wt % did not adversely affect the electrochemical reaction.

A summary of commercial processes for the manufacture of MEK is provided by Baiel *et al.* [18]. Manufacture of MEK is currently carried out by vapour phase catalytic dehydrogenation of 2-butanol produced from 1-butene either by indirect hydration in sulphuric acid or by direct hydration over an acidic ion-exchange resin or a solution of tungsten.

$$C_4H_{8(g)} + H_2O_{(l)} \rightarrow C_4H_{10}O_{(l)}$$

MEK is subsequently obtained by catalytic dehydrogenation of 2-butanol in the vapour phase over ZnO

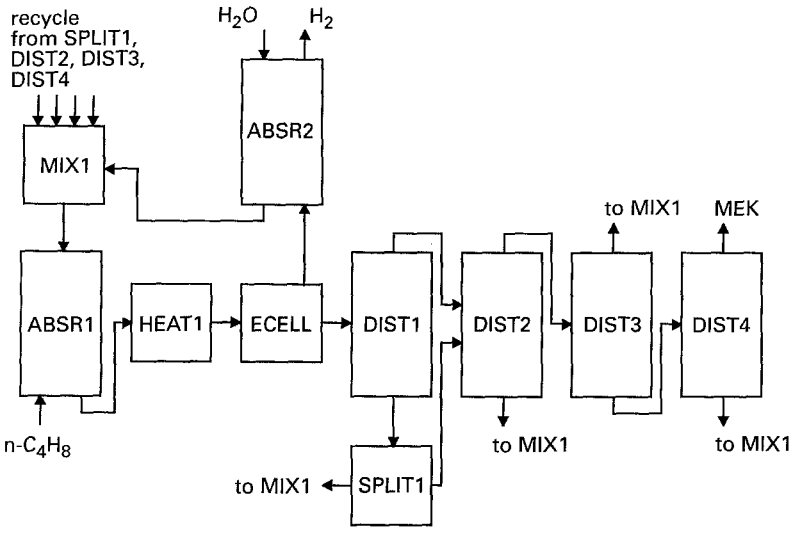

Fig. 3. Aspen flowsheet module representation for MEK liquor recovery process.

or brass at elevated temperature (616–755 K) and pressure (103–310 kPa). At the time of this analysis, the selling price of commercial commodity MEK in the US was \$63 $kmol^{-1}$.

2.2. *Process flowsheeting*

At the inception of this study, no general-purpose commercial flowsheeting package was available for handling electrolytes and for optimization; packages with these capabilities are now available as mentioned above. The present investigation employed the Aspen flowsheeting package [19], enhanced by the use of electrolytic modelling procedures developed by Cera [20] and La Roche [2] and simultaneous-modular optimization techniques developed by Chen and Stadtherr [21–23].

Figures 3 and 4 illustrate Aspen flowsheets for the liquor recovery and gas recovery processes, respectively. The butene absorber (ABSR1) was modelled by an equilibrium reactor module since the overall reaction was reported to be a second order reaction that went very rapidly to equilibrium [17]. The heat of reaction was used to preheat the cell feed. The Aspen program contained unit modules for simulating an equilibrium reactor (REQUIL), multistage distillation (RADFRC), vapour–liquid equilibrium flash separator (FLASH2), liquid flow splitter (FSPLIT), heater (HEATER), and mixer (MIXER). A user-supplied module (USER) was developed for the electrolytic cell based on the best cell operating conditions described by Worsham and coworkers. The first distillation separates a MEK/2-butanol/water mixture near the MEK/water azeotrope (66% MEK) from the sulphuric acid. The second distillation serves to dry the mixture by addition of sulphuric acid at the top of the column. A MEK/2-butanol stream with trace water is taken overhead to the third column which removes a MEK/water azeotrope from the MEK/2-butanol. The finishing column achieves 99% MEK product by removing 2-butanol.

The Aspen module specifications for the flowsheets given in Figs 3 and 4 are provided in Tables 1 and 2. Additional process details along with the temperature and composition of all streams are available elsewhere [2]. The tables also indicate decision variables (conversion and boil-up ratios) which are to be determined by the optimization.

3. Physical property modelling

An auxiliary data bank was created within the Aspen code for the properties of ionic species present in the MEK flowsheets. These included aqueous heat of formation, aqueous free energy of formation, ionic charge, molecular weight, and standard state

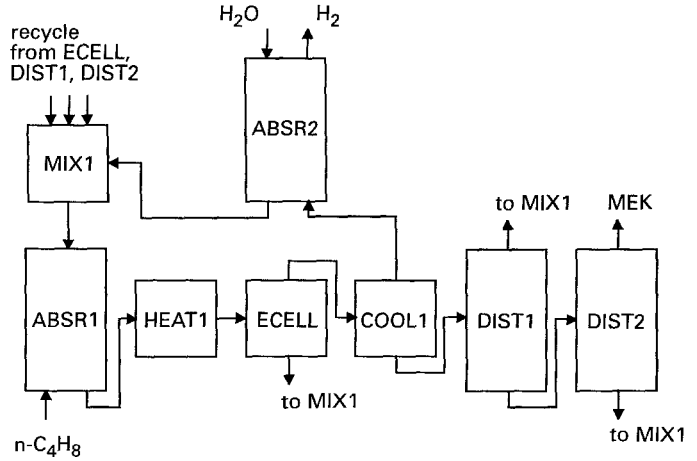

Fig. 4. Aspen flowsheet module representation for MEK gas recovery process.

Table 1. Aspen module specifications for MEK cell liquor recovery

	Temperature K	*Pressure* kPa	*Decision variable*
Electrolytic reactor ECELL	350	206.8	Conversion
Cell gas absorber (ammonia refrigerant) ABSR2	278	101.3	
Distillation 1 DIST1		101.3	Boil-up ratio
Flow splitter SPLIT1			Split fraction
Distillation 2 DIST2		101.3	Boil-up ratio
Distillation 3 DIST3		101.3	Boil-up ratio
Distillation 4 DIST4		101.3	Boil-up ratio
Mixer MIX1		101.3	
1-Butene absorber ABSR1	333	689.3	
Cell feed heater HEAT1	350	482.5	

Table 2. Aspen module specifications for MEK cell gas recovery

	Temperature K	*Pressure* kPa	*Decision variable*
Electrolytic reactor ECELL	350	206.8	Conversion
Cell gas condenser (ammonia refrigerant) COOL1	278	101.3	
Cell gas absorber ABSR2	278	101.3	
Distillation 1 DIST1		101.3	Boil-up ratio
Distillation 2 DIST2		101.3	Boil-up ratio
Mixer MIX1		101.3	
1-Butene absorber ABSR1	333	689.3	
Cell feed heater HEAT1	350	482.5	

entropy. National Bureau of Standards compilations of data [24] and bibliography of data sources [25] were used.

The Redlich–Kwong equation of state was chosen for predicting the vapour properties of both flowsheets. The non–random two-liquid (NRTL) model was used for liquid mixture properties in areas of the flowsheets that did not contain electrolytes.

The electrolyte NRTL model [12] was used to predict activity coefficients for the vapour–liquid equilibrium calculations in flowsheet sections that involved electrolytic solutions. Long-range ionic forces were predicted with the Debye–Huckel–Pitzer method, and short-range forces were modelled by the local composition approach of the NRTL model [26]. The binary parameters for each solvent–ion and solvent–solvent pair in the MEK system were obtained by regression of vapour–liquid equilibrium data [8] from which activity coefficients were predicted and used to determine vapour–liquid equilibria.

4. Flowsheet specifications

Product purity was set at 99 mol % MEK, a typical commercial product specification. Electrochemical cell performance was based on the best operating conditions with respect to current density: 1292 A m^{-2} at 350 K. High current efficiency (100%) was reported at 1.65 V and up to 20% conversion per pass. The current density dependence was not reported in the patents. As suggested in the patents, the cell feed acid concentration was set at 65 wt % H_2SO_4, and the mole ratio of H^+ to butanol in the cell feed was maintained at 1 : 1. In addition, the MEK concentration was constrained to be no more than 22 mol % in the cell liquid. These constraints were also used in the optimization of both flowsheets.

5. Process optimization

The optimization study was formulated as a nonlinear programming (NLP) problem where one seeks to minimize an objective function subject to a set of inequality and equality constraints. The objective function in the present study was to minimize the MEK selling price required to achieve a 20% discounted cash flow rate of return (DCFRR).

Table 3 indicates the values of principal parameters used in the economic analysis. For the electrolytic section, procedures for estimating capital and operating costs were based on the factored approach to electroorganic plant cost estimation [27] as summarized in Table 4. For remaining units in the flowsheet, ASPEN cost routines were used for estimating the capital cost of pumps, heat exchangers, absorber, and distillation columns.

For each flow configuration, the decision variables were chosen to be the cell feed stream variables, 1-butene feed flow, water feed flow, plant size, electrolytic cell conversion per pass, and distillation boil-up ratios (the mole ratio of reboiler vapour rate to the bottoms liquid rate). In addition, the liquor recovery flowsheet had the split fraction (from unit SPLIT1) as a decision variable. The current density was not selected as a decision variable because data were not available for the relation between current density and current efficiency.

As a framework for the optimization, a simultaneous-modular [21–23] interface was written for an Aspen-based flowsheeting system. This allowed tear stream and design specification equations to be considered simultaneously at the flowsheet level. This set of equations became part of a nonlinear programming (NLP) problem for which the independent variables were chosen to be the tear stream and decision variables of the flowsheet. The constraints

Table 3. Economic parameters used for optimization

Plant life	10 years
Plant availability	8000 h y^{-1}
Construction period	2 years
Tax rate	46%
Electricity	0.035 \$ kWh^{-1}
Steam (100 psig)	0.0138 \$ kWh^{-1}
Cooling water	0.00222 \$ kWh^{-1}
Ammonia refrigeration	0.0190 \$ kWh^{-1}
N-butene	0.573 \$ kg^{-1}
Process water	0.283 \$ $kton^{-1}$
Hydrogen	0.308 \$ kg^{-1}

Table 4. Economic relationships used for synthesis plants

Capital items	
Cells	$A_c = 3750\,\$\,cell^{-1}$
Rectifiers	$A_R = 0.07\,\$\,W^{-1}$
Heat exchangers	$^*A_H = 4500\,\$\,m^{-2}$
Pumps	$^*A_p = 90\,\$\,s\,l^{-1}$
	$a = 1.0$
Tanks	$^*A_T = 200\,\$\,l^{-0.5}$
	$\theta_T = 40\,s$
Electrolysis	$L_C = 4.0$
Capital	$L_R = 2.5$
	$L_A = 5.0$
Operating costs	
Electricity	$A_e = 0.035\,\$\,kWh^{-1}$
	$H = 8000\,h\,y^{-1}$
	$\epsilon_R = 0.98$
Cooling water	$A_{cw} = 0.023\,\$\,m^{-3}$
Cell maintenance $C_{cm} = A_{cm} I_{TOT}$	$A_{cm} = 0.2\,\$\,A^{-1}\,y^{-1}$
Other maintenance $C_{om} = A_{om}(C_{TOT} - C_C)$	$A_{om} = 0.04\,y^{-1}$
Cell labour $C_{cl} = A_{cl} N$	$A_{cl} = 700\,\$\,cell^{-1}\,y^{-1}$

* Equipment based on 304 stainless steel.

consisted of the tear stream and design specification equations along with any independent variable bounds. Full documentation of the input file is available in Appendix C of [2].

The cell feed was chosen as the tear stream for both configurations. For the liquor recovery flowsheet, the order in which calculations were carried out was ECELL, ABSR2, DIST1, SPLIT1, DIST2, DIST3, DIST4, MIX1, ABSR1, and HEAT1. For the gas recovery process, the order of calculations was ECELL, COOL1, ABSR2, DIST1, DIST2, MIX1, ABSR1, and HEAT1. The flowsheet Jacobian was calculated by the full-block perturbation method for the direct difference approximation [21].

A modified Han–Powell successive quadratic programming algorithm, SQPHP [21–23], was used to solve the optimization problem. The interface between SQPHP and Aspen was accomplished through use of Aspen Fortran blocks and Fortran subroutines. These interface subroutines were written in a general manner to allow optimization capability for any Aspen-based flowsheeting system [2]. Successive quadratic programming (SQP) methods [28, 29] were used to conserve computation time by following an infeasible path approach to the optimum. When reliability problems surfaced during the computation, usually appearing as line search failures, the alternative line search strategy method of Chen and Stadtherr [29] was used; the program also incorporated as an option the partial Broyden convergence scheme [30]. The optimum was considered to have been identified when the weighted sum of the possible objective function improvement and constraint violations was less than a specified tolerance. Lagrangian multipliers obtained as a result of the optimization were used to identify key process variables to which the optimum was most sensitive.

5.1. *Computation requirements*

Calculations were performed in an IBM 3081-GX mainframe. For both flowsheets, two sequential-modular initialization iterations with Aspen were used before proceeding to the simultaneous-modular SQPHP optimization phase.

The liquor recovery process required 8 SQPHP optimization iterations for a total of 18.4 CPU minutes. It was found that this was 5.8 times the computer time required to do a simulation (non-optimization) calculation with the same initial guesses for the decision variables. The gas recovery process optimization run took 3.1 CPU minutes with 8 SQPHP iterations, and was 2.4 times the comparable simulation run time. The computational time associated with the liquor recovery process was longer owing to the complexities associated with the electrolyte distillations.

6. Results and discussion

6.1. *Liquor recovery process*

Table 5 summarizes results for the liquor recovery process flowsheet. The optimal plant size for this process was found to be 34.0 kton y^{-1} for which the minimum selling price was \$85.9 $kmol^{-1}$. An increase in plant size toward the upper bound of 45 kton y^{-1} was found to be counterproductive owing to increased distillation costs. Table 5 also illustrates the breakdown of capital costs for the optimal liquor recovery flowsheet. Nearly two-thirds of the capital was invested in the product recovery section of which the first two distillations, which handle large electrolyte streams, accounted for the most significant portion.

Annual operating costs, shown in Table 5, were \$18.4 × 10^6 y^{-1} of which the electrolytic section consumed about three-fourths owing primarily to power costs. It may be seen that two of the distillation units were energy intensive because of the need to vapourize and condense large aqueous streams. The finishing column was energy intensive because of the need to boost column reflux to achieve 99 mol % product purity.

The optimal values for the design variables are indicated on the lower left side of Table 5. Sensitivity results, shown in the lower right side of Table 5, provided quantitative information on the relative importance of the operating parameters. For

Table 5. Gas recovery process

Capacity	$34\ \text{kton y}^{-1}$		
Selling price	$\$86\ \text{kmol}^{-1}$		
		Capital cost	*Operating costs*
Total		$\$15.6 \times 10^6$	$\$18.4 \times 10^6\ \text{y}^{-1}$
Breakdown by process unit			
Electrolyte cell		36.3%	77.7%
Distillation 1		31.4	7.7
Distillation 2		21.3	5.0
Distillation 3		3.6	0.6
Distillation 4		5.1	7.0
Absorbers		2.3	2.0
Design variables	*Optimal value*	*Limits*	*Sensitivity* ($/kmol % change)
n-Butene feed flow	$0.017\ \text{kmol s}^{-1}$	0.0001–0.0250	−0.453
Reactor conversion	0.20	0.01–0.20	−0.063
Waterfeed flow	$0.016\ \text{kmol s}^{-1}$	0.0001–0.030	−0.33
DIST1 boil-up ratio	0.55	0.1–100	+0.027
SPLIT1 split fraction	0.50	0.1–0.50	+0.034
DIST2 boil-up ratio	0.68	0.1–100	+2.02
DIST3 boil-up ratio	0.62	0.1–100	−0.31
DIST4 boil-up ratio	4.4	0.1–100	+0.57

example, holding other decision variables constant, an incremental increase in butene flow rate extrapolated to 1% would decrease the MEK price by $\$0.453\ \text{kmol}^{-1}$. The results indicated that useful directions for further process improvement would be to increase butene feed flow, the water feed flow, and the boilup ratio of distillation column 3; and to decrease the boilup ratios in columns 2 and 4. The results provided in Table 5 also suggest that research directed toward releasing the need for high sulphuric acid concentration and a 1 : 1 feedstock ratio could improve process economics.

It is also seen in Table 5 that the optimum values (second column) of the reactor conversion (0.20) and the split fraction (0.50) are at the limit (third column) but that the sensitivity coefficients (fourth column) are low so that the limits would have to be changed significantly if they were to have a significant effect on the economics.

Based on the commercial commodity MEK price at the time of this analysis ($\$63\ \text{kmol}^{-1}$), the optimal liquor recovery process described above was found (at $\$89.5\ \text{kmol}^{-1}$) to be not economically viable.

6.2. *Gas recovery process*

Table 6 provides capital costs, operating costs, and sensitivity analysis of the optimum gas recovery process. The MEK selling price of $\$58.1\ \text{kmol}^{-1}$ was marginally competitive with the prevailing market price of $\$63\ \text{kmol}^{-1}$.

The capital investment for the gas recovery process was $\$12.1 \times 10^6$, a reduction by about 20% from the liquor recovery process. The optimal plant size was found to be $44.7\ \text{kton y}^{-1}$, or about 30% higher than the liquor recovery process. It may be seen that the electrolytic section represented over 80% of the total capital costs.

Table 6 indicates that the annual operating costs for the gas recovery process were $\$27.2 \times 10^6\ \text{y}^{-1}$ primarily for electrolytic power and for absorber refrigeration for condensing MEK product from the

Table 6. Liquor recovery process

Capacity	$45\ \text{kton y}^{-1}$		
Selling price	$\$58\ \text{kmol}^{-1}$		
		Capital cost	*Operating costs*
Total		$\$12.1 \times 10^6$	$\$27.2 \times 10^6\ \text{y}^{-1}$
Breakdown by process unit			
Electrolytic cell		83.5%	88.9%
Distillation 1		5.0	0.5
Distillation 2		7.5	1.8
Absorbers		2.2	8.9
Design variables	*Optimal value*	*Limits*	*Sensitivity* ($/kmol % change)
n-Butene feed flow	$0.022\ \text{kmol s}^{-1}$	0.0001–0.0250	+0.033
Reactor conversion	0.20	0.01–0.20	−0.20
Waterfeed flow	$0.023\ \text{kmol s}^{-1}$	0.0001–0.030	−0.024
DIST1 boil-up ratio	1.1	0.3–100	+0.54
DIST2 boil-up ratio	8.0	3.0–100	+0.033

cell gas. Product recovery operating costs were only 2.3% of the total.

The lower portion of Table 6 provides sensitivity results for the gas recovery process. By comparison with the liquid recovery process, it may be recognized that the percent conversion in the electrolytic reaction was a more significant variable; a 1% increase in conversion would decrease MEK selling price by \$0.20 $kmol^{-1}$. Since the optimum was found to coincide with the 20% conversion constraint indicated in the patents, and since the optimum was sensitive to this variable, it may be concluded that improvements in cell design that would increase conversion per pass should be explored.

Evaluation of the role of the current density was not carried out owing to lack of pilot-plant data as noted previously. To do this would be straightforward once data were available.

7. Conclusions

Optimization of electrolytic process flowsheets was carried out by a simultaneous-modular method which utilized the public version of the Aspen flowsheeting package along with an algebraic model of the electrolytic cell and electrolyte physical property data. The test cases included azeotropic distillation and distillation of electrolytic solutions. The optimizations were carried out by an infeasible path method based on successive quadratic programming methods. The optimization calculations took only two to six times longer than corresponding simulation runs. Computer execution time depended strongly on the complexity of the distillation units. An analysis of sensitivity of the optimum to process variables was carried out by examination of the Lagrangian multipliers of the constraint equations. The method of evaluation is generic and could incorporate other process chemistries as well as more refined process data, more detailed process flowsheets, and more sophisticated mathematical models of electrolytic cells.

Two case studies on electrosynthesis of methyl ethyl ketone from 1-butene were investigated based on process information provided in the patent literature. In the liquor recovery process, MEK was separated from cell liquor by a series of four distillations which were made complicated by the presence of an azeotrope. In the gas recovery process, MEK was separated by condensation of cell gas. Although neither of the case studies gave promising results from a commercial point of view, the method of evaluation was found to be robust.

Acknowledgements

This investigation was supported by Dow Chemical Company. During the course of the study, RL held fellowships sponsored by Amoco, Chevron and Shell.

References

[1] J. Douglas, 'Conceptual Design of Chemical Processes', McGraw-Hill, New York (1988).
[2] R. La Roche, Ph.D thesis, Department of Chemical Engineering, University of Illinois at Urbana-Champaign (1988).
[3] R. Alkire, G. Cera and M. Stadtherr, *J. Electrochem. Soc.* **129** (1982) 1225.
[4] R. Alkire, S-A. Soon and M. Stadtherr, *ibid.* **132** (1985) 1105.
[5] C. King, *in* 'Tutorial Lectures in Electrochemical Engineering and Technology', (edited by R. Alkire and D. Chin), *AIChE Symposium Ser.* **229:79** (1983) 79.
[6] M. Krumpelt, E. Weissman and R. Alkire (Eds), 'Electroorganic Synthesis Technology', *AIChE Symposium Ser.* **185** (1979) 75.
[7] R. Plimley, *J. Chem. Tech. Biotechnol.* **30** (1980) 233.
[8] R. Alkire, R. La Roche, G. Cera and M. Stadtherr, *J. Electrochem. Soc.* **133** (1986) 290.
[9] R. La Roche, O. Araujo, R. Alkire and M. Stadtherr, 'Computer aided process optimization for indirect electrosynthesis of 1,4-naphthoquinone', submitted to *J. Electrochem. Soc.*
[10] R. Alkire and O. Araujo, *J. Electrochem. Soc.* **139** (1992) 737.
[11] R. Reid, J. Prausnitz and B. Poling. 'The Properties of Gases and Liquids', 4th edn. McGraw-Hill, New York (1987).
[12] C-C. Chen, H. Britt, J. Boston and L. Evans, *AIChE J.* **25** (1979) 820.
[13] C. Worsham, *US Patent 3 247 084* (1966).
[14] L. Griffin, J. Clarke and C. Worsham, *US Patent 3 329 593* (1967).
[15] T. Beck, R. Alkire, N. Weinberg, R. Ruggeri and M. Stadtherr, *in* 'Techniques of Electroorganic Synthesis', Vol. 3 (edited by N. Weinberg and B. Tilak), Willey-Interscience, New York (1982) p. 423.
[16] S. Swann, Jr. and R. Alkire, 'Bibliography of Electroorganic Syntheses, 1801–1975', The Electrochemical Society, Pennington, NJ (1980).
[17] D. Sankholkar and M. Sharma, *Chem. Eng. Sci.* **28** (1973) 49.
[18] J. Baiel, C. Savini, and J. Stanat, *in* 'Encyclopedia of Chemical Processing and Design', Vol. 30 (edited by J. McKetta and W. Cunningham), Marcel Dekker, New York (1989) p. 32.
[19] L. Evans, J. Boston, H. Britt, P. Gallier, P. Gupta, B. Joseph, V. Mahelec, E. Ng, W. Seider and H. Yagi, *Comput. Chem. Eng.* **3** (1979) 319.
[20] G. Cera, Ph.D thesis, Department of Chemical Engineering, University of Illinois, Urbana, IL (1983).
[21] H-S. Chen and M. Stadtherr, *AIChE J.* **31** (1985) 1843.
[22] *Idem, ibid.* **31** (1985) 1857.
[23] *Idem, ibid.* **31** (1985) 1868.
[24] D. Wagman, W. Evans, V. Parker, R. Schumm, I. Halow, S. Bailey, K. Churney and R. Nuttal, 'The NBS Tables of Chemical Thermodynamic Properties: Selected Values for Inorganic and C1 and C2 Organic Substances in SI Units', American Institute of Physics, New York (1982).
[25] R. Goldberg, 'Compiled Thermodynamic Data Sources for Aqueous and Biochemical Systems: An Annotated Bibliography (1930–1983)', NBS Special Publication 685, National Bureau of Standards, Gaithersburg, MD (1984).
[26] H. Renon and J. Prausnitz, *AIChE J.* **14** (1968) 135.
[27] D. Danley, 'Emerging Opportunities for Electroorganic Processes', Marcel Dekker, New York (1984).
[28] L. Biegler and J. Cuthrell, *Comput. Chem. Eng.* **9** (1985) 257.
[29] H-S. Chen and M. Stadtherr, *ibid.* **8** (1984) 229.
[30] Y-D. Lang and L. Biegler, *ibid.* **12** (1987) 143.